TAO, Vol. 10, No. 1, 201-214, March 1999

Authigenic Uranium in Marine Sediments of the Benguela Current Upwelling Region During the Last Glacial Period

Ein-Fen Yu[1], Chih-Hung Liang[1] and Min-Te Chen[2]

(Manuscript received 9 November 1998, in final form 5 February 1999)

ABSTRACT

Anomalously high uranium contents and $^{238}U/^{232}Th$ activity ratios deposited during the oxygen isotope stages 2 to 4 are observed in the MD962085 core from the Benguela Current upwelling area. In conjunction with the activity ratio of $^{234}U/^{238}U$, the high uranium contents found in this core cannot be considered as detrital; instead, they must be of authigenic origin. The high biological productivity in the overlying seawater may have induced a high flux of organic matter resulting, directly or indirectly, in a reducing environment, and may have led to the addition of authigenic uranium to the sediments during the last glacial period. The correspondence between the variations in authigenic U content, %TOC, and $^{230}Th_{ex}$-normalized TOC flux supports this suggestion. The observed high paleoproductivity during the last glacial period of the core may be due to the greater intensity of upwelling in the Benguela Current upwelling system.

(Key words: Authigenic uranium, Last glacial stage, Benguela Current upwelling)

1. INTRODUCTION

Th and U isotopes, and TOC content in a gravity core were measured to examine the diagenetic behavior of uranium in the Benguela Current upwelling region. The core was collected by R/V*Marion Dufresne* during the IMAGES (International Marine Past Global Changes Study Program) II cruise.

Uranium and its daughters have been shown to be valuable as geochronometers (e.g. Broecker and Peng, 1982; Bard et al., 1990) and paleoceanographic proxies (e.g. Francois et al., 1993; Yu et al., 1996), resulting in intensive study of the marine geochemistry of uranium for decades (Cochran and Krishnaswami, 1980; Anderson, 1982; Colley and Thomson, 1985; Cochran et al., 1986; Wallace et al., 1988; Anderson et al., 1989; Barnes and Cochran, 1990;

[1]Department of Earth Sciences, National Taiwan Normal University, Taipei, Taiwan, ROC
[2]Institute of Applied Geophysics, National Taiwan Ocean University, Keelung, Taiwan, ROC

Klinkhammer and Palmer, 1991). These studies have suggested that uranium behaves conservatively with the formation of soluble U(VI) carbonate complexes in oxygenated seawater; however, under reducing conditions soluble U(VI) in the overlying seawater can be transformed into insoluble U(IV). This transformation, which can occur in the seawater column, at the sediment-water interface, and within the sediments, resulted in the addition of authigenic uranium to sediments, and altered the uranium distribution in the sedimentary records.

It became clear that uranium is reactive in some marine environments such as anoxic basins (e.g. Anderson, 1989), coastal oceans (e.g. Cochran et al., 1986), turbidites (e.g. Colley and Thomson, 1985) and pelagic sediments (e.g. Wallace et al., 1988). For sediments in upwelling areas, a relatively high flux of particulate organic matter can easily make the regions suboxic or anoxic environments; uranium is thus easily able to behave unconservatively. This paper adds detail to current knowledge on the behavior of dissolved uranium in sediments of the Benguela Current upwelling region, and also examines how the uranium distribution in the sedimentary records corresponds to the variations of the ocean conditions in the region with the glacial to interglacial climate changes.

The surface water layer at the core site is strongly influenced by the Benguela Current, which flows northward along the southwest African coast mainly between 34 °S and 15 °S (Nelson and Hutchings, 1983). This northward flow begins to bend northwest and flows away from the coast at about latitude 30 °S (Nelson and Hutchings, 1983; Stramma and Peterson, 1989; Figure 1). To the west, this part of the current is juxtaposed to the coastal current from the geostrophic current of the South Atlantic anticyclonic gyre (Stramma and Peterson, 1989). Due to the prevailing wind, the coastal upwelling develops within the easternmost section of the Benguela Current, which has been referred to as the Benguela Current upwelling system (Shannon, 1985).

Paleontological and sedimentological studies have shown that the upwelling activity of the Benguela Current region has existed for millions of years (Siesser, 1978; Diester-Haass, 1985; Oberhansli, 1991). The intensity and distribution of Benguela Current upwelling system are important not only to surface area of the high productivity zone and in attendant fluxes of sedimentary materials to the seafloor, but also to the amount of upwelled cool, nutrient-rich and O_2-depleted waters. All of these variations are important factors which affect the diagenetic behavior of uranium in the sediments.

2. MATERIAL AND METHODS

2.1 Sample Material

The MD962085 core was sampled at 29°42'S, 12°56'E in a water depth of 3001 m (Figure 1). The site is located off the coast of the Orange River where the surface water layer is strongly influenced by the Benguela Current upwelling system. The core is 35.4 m in length, but only the first 4 meters has been analyzed and discussed. The data represent the whole last glacial period from oxygen isotopic stages 2 to 4 to the present time. To provide a high-resolution record, most of the core was sampled at intervals of 5-10 cm, which represented a frequency of approximately 1 to 2 kyr.

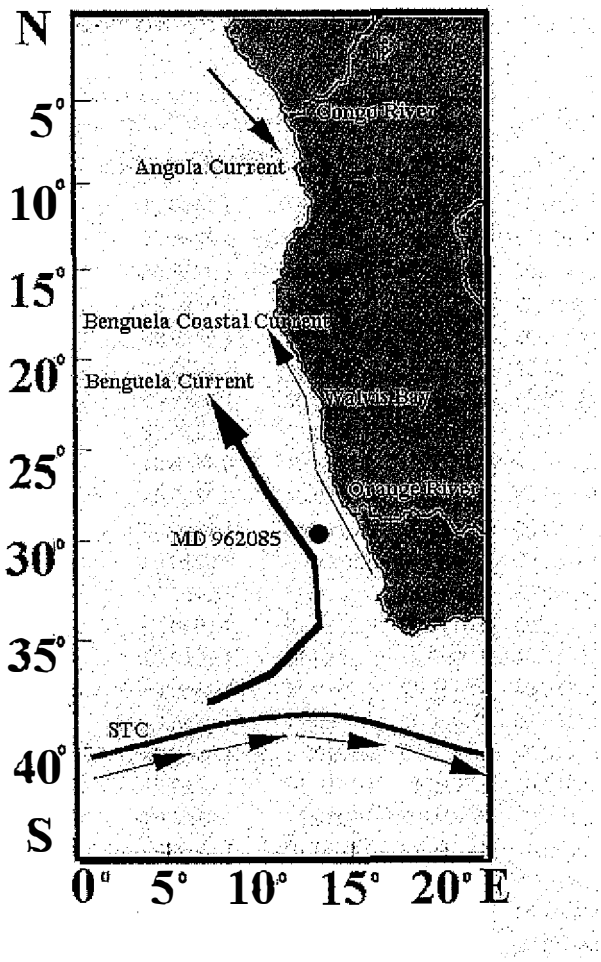

Fig. 1. Location of the MD962085 core, and schematic diagram of main features of the Benguela Current upwelling system and subtropical convergence (STC).

2.2 Analytical Procedures

Analysis of Th and U isotopes -All samples were subjected to total dissolution with mixtures of HNO_3, HF, and $HClO_4$ in the presence of ^{236}U and ^{229}Th as yield monitors. The radiochemical analyses followed the method of Anderson and Fleer (1982) with some modifications. Briefly, Th isotopes were separated from U isotopes by elution with 9N HCl from AG1-X8 anion exchange resin; after Th elution, U isotopes were eluted with dilute HCl. Both Th and U solutions were evaporated to near dryness, put into 8N HNO_3, and purified separately by using an 8N HNO_3 anion exchange column. The recovered Th and U solutions were evaporated separately to a small drop of concentrated HNO_3 and taken up in 0.01M HNO_3 and 2M NH_4Cl before electroplating. Th and U isotopes were determined by counting emitted alpha-particles with silicon surface-barrier detectors. The analytical precision (1 σ) is reported in Table 1.

The final uncertainties of the radioisotope analyses in Table 1 are from several sources. The primary contribution is from the number of raw counts of spectra for individual isotopes. Other factors, such as background and decay correction and low sample weight, also affect the

Table 1. ^{238}U and ^{232}Th activities, and $^{234}U/^{238}U$ activity ratio of the MD962085 core.

Sample depth (cm)	C-14 age (ka)	O-18 age (ka)	Th-230 dpm/g	Th-232 dpm/g	U-238 dpm/g	U-234 dpm/g	U-234/U-238 (dpm/g)/(dpm/g)	% authigenic U
3.5	3.97	1.00	7.64±0.18	0.41±0.03	0.35±0.02	0.40±0.03	1.14±0.11	0.06
8.5	4.42	2.43	7.05±0.13	0.42±0.02	0.42±0.02	0.51±0.03	1.21±0.09	0.20
13.5	4.87	3.86	7.16±0.14	0.44±0.02	0.64±0.02	0.70±0.03	1.09±0.06	0.45
18.5	5.32	5.29	7.04±0.19	0.37±0.03	0.32±0.01	0.33±0.02	1.03±0.07	0.08
23.5	6.01	6.25	6.67±0.18	0.43±0.03	0.29±0.01	0.31±0.02	1.07±0.08	0.00
33.5	7.39	7.25	6.69±0.15	0.58±0.03	0.53±0.04	0.55±0.04	1.04±0.11	0.12
43.5	8.77	8.25	6.30±0.12	0.41±0.02	0.33±0.01	0.34±0.02	1.03±0.07	0.01
53.5	10.16	9.25	6.66±0.15	0.42±0.02	0.29±0.01	0.32±0.02	1.10±0.08	0.00
63.5	11.54	10.25	6.79±0.17	0.51±0.03	0.34±0.01	0.32±0.01	0.94±0.04	0.00
68.5	12.23	10.75	6.54±0.14	0.38±0.03	0.35±0.01	0.34±0.02	0.97±0.08	0.13
73.5	12.92	11.25	7.09±0.15	0.50±0.02	0.61±0.02	0.67±0.02	1.10±0.05	0.34
78.5	13.51	11.75	6.71±0.09	0.54±0.02	2.84±0.10	3.02±0.01	1.06±0.05	0.85
83.5	14.11	12.64	6.92±0.16	0.53±0.03	3.22±0.11	3.44±0.12	1.07±0.05	0.87
103.5	16.95	13.91	6.40±0.09	0.59±0.03	2.61±0.09	2.86±0.10	1.10±0.05	0.82
108.5	17.66	19.00	5.86±0.18	0.50±0.04	2.99±0.09	3.30±0.10	1.10±0.05	0.87
113.5		19.91	6.87±0.21	0.55±0.04	4.21±0.12	4.76±0.14	1.13±0.05	0.90
118.5		20.82	6.01±0.24	0.52±0.05	3.03±0.12	3.49±0.14	1.15±0.06	0.86
123.5		21.73	6.30±0.19	0.52±0.04	2.94±0.09	3.19±0.10	1.09±0.05	0.86
128.5		22.64	6.41±0.24	0.60±0.05	2.89±0.12	3.16±0.14	1.09±0.07	0.83
133.5		23.55	6.78±0.14	0.61±0.03	2.86±0.07	3.10±0.09	1.08±0.04	0.83
138.5		24.44	6.65±0.17	0.67±0.04	3.40±0.13	3.69±0.14	1.09±0.05	0.84
148.5		26.22	5.72±0.22	0.57±0.05	1.91±0.10	2.24±0.11	1.17±0.08	0.76
153.5		27.11	6.29±0.19	0.38±0.03	1.90±0.10	2.14±0.11	1.13±0.08	0.84
158.5		28.00	6.30±0.24	0.60±0.06	1.92±0.09	2.08±0.10	1.08±0.07	0.75
173.5		31.00	6.62±0.13	0.56±0.03	2.83±0.10	3.15±0.11	1.11±0.06	0.84
183.5		33.00	6.56±0.15	0.63±0.03	4.42±0.22	4.97±0.25	1.12±0.08	0.89
213.5		39.00	5.92±0.16	0.52±0.03	4.00±0.21	4.45±0.24	1.11±0.08	0.90
223.5		41.00	5.09±0.16	0.45±0.04	3.14±0.14	3.53±0.16	1.12±0.07	0.89
233.5		43.00	5.63±0.15	0.58±0.03	2.44±0.07	2.71±0.07	1.11±0.04	0.81
263.5		49.00	5.24±0.16	0.52±0.03	2.50±0.10	2.87±0.11	1.15±0.06	0.83
273.5		51.00	4.84±0.09	0.52±0.02	2.47±0.08	2.83±0.10	1.15±0.05	0.83
283.5		53.00	5.09±0.10	0.50±0.03	2.90±0.10	3.43±0.12	1.18±0.06	0.86
288.5		53.92	4.80±0.22	0.48±0.05	2.36±0.10	2.75±0.11	1.17±0.07	0.84
293.5		54.85	5.24±0.22	0.52±0.05	2.35±0.10	2.36±0.11	1.00±0.06	0.82
333.5		62.23	4.77±0.13	0.73±0.04	2.00±0.07	2.20±0.08	1.10±0.06	0.71
343.5		64.08	4.91±0.13	0.83±0.04	2.17±0.07	2.40±0.08	1.11±0.05	0.69
353.5		66.25	5.59±0.13	0.74±0.04	3.20±0.12	3.47±0.13	1.08±0.06	0.82
363.5		68.75	5.68±0.12	0.82±0.44	3.99±0.16	4.21±0.17	1.06±0.06	0.84
373.5		71.25	2.77±0.08	0.54±0.03	1.17±0.05	1.24±0.06	1.06±0.06	0.63
403.5		78.75	4.49±0.13	0.71±0.04	2.46±0.13	2.66±0.14	1.08±0.08	0.77
423.5		81.62	4.54±0.14	0.62±0.04	2.92±0.16	3.43±0.09	1.17±0.09	0.83

final uncertainties. Additional uncertainties for calculating radioactivity ratio are included the propagation of all sources of errors, which is discussed in detail by Ku (1966). The activities of U and Th isotopes are calculated from the raw counts for the isotope in a given peak area and are subtracted from the number of background counts. For ^{238}U, ^{236}U, and ^{234}U, the peak area of each isotope includes the same number of channels because the shape of the spectra for all U isotopes. For ^{232}Th, ^{230}Th and ^{229}Th, the shapes of the spectra are different for each isotopes. The number of counts of the two channels on the two sides of each Th peak area was taken account for 0.5% of the total integrated counts in the peak area. The background correction was made taking the number of the background counts to be equal to that in the same area (with the same number of channels) of each peak area of the isotope. For ^{230}Th and ^{229}Th isotopes, the largest sources of background were generally from low energy tailing counts of higher energy isotopes. Therefore, tail correction was combined with background correction. For more details, refer to Yu (1994).

Organic Carbon-Total carbon and organic carbon content were determined using a HORIBA carbon/sulfur analyzer. The analytical procedure from Hedges and Stern (1984) and Chang et al. (1991) was followed. A preweighed sample of 0.07-0.1 g was first analyzed for total carbon content using the analyzer, and was then treated with fuming HCl to leach out the inorganic carbon and thus allow the analysis of organic carbon. After the fuming HCl acidification, the carbon content determined is defined as the content of organic carbon. The fuming HCl acidification was suggested as the best method to remove carbonate from marine sediments (Chang et al., 1991). Replicate measurements of a standard for total carbon analyses give an average value of 0.673±0.005 %C (1 σ, n=5) with an accuracy of ± 0.03%. The blanks for total carbon ranged from 0.002 to 0.004%C.

AMS ^{14}C dating-The monospecific samples of *G. inflata* of several sections of the core were used to generate the AMS ^{14}C age. The monospecific samples of *G. inflata* were handpicked from the dry coarse fraction, >63 mm size. Foraminifera were ultrasonically cleaned using methanol to remove adhering particles, followed by soaking in a solution of 5% NaClO for 12 hours. The cleaned foraminifera samples were converted into CO_2 gases and collected via vacuum line in the stable isotope laboratory of the Institute of Earth Sciences, Academia Sinica, Taipei. The radiocarbon measurements of the CO_2 gas samples were made by the Rafter Radiocarbon Laboratory at the Institute of Geological and Nuclear Sciences in New Zealand. The AMS ^{14}C dates are calculated conventionally (i.e., relative to 0.95 National Bureau of Standards oxalic acid using the Libby half-life of 5568 years). The data of core MD962085 are available electronically at Paleoceanographic Data Center of Core Laboratory-Center for Ocean Research, NSC, at the Institute of Applied Geophysics, National Taiwan Ocean University, Keelung, Taiwan, R.O.C. (Internet:http://140.121.175.114).

3. RESULTS AND DISCUSSION

3.1 Age Model and Sedimentation Rates

Age model for the MD962085 core was established by both radiocarbon dating and oxygen isotope stratigraphy. No correction was made for the difference in $^{14}C/^{12}C$ ratios between

surface ocean ΣCO_2 and atmospheric CO_2 for the AMS ^{14}C ages. This correction is currently about 400 years for most places in the surface ocean (Broecker et al., 1988). However, the AMS ^{14}C ages established for MD962085 were converted into calendar ages based on CALIB 3.03C (Stuiver and Reimer, 1993), a program used to calibrate ^{14}C ages with respective to tree-rings. Table 1 lists the calculated model ages for the top 110 cm of the core which is developed on the basis of linear interpolation between adjacent calibrated radiocarbon dates.

Since no AMS ^{14}C data are available below the top 110 cm, oxygen isotope was employed as the stratigraphic framework for deeper sections of the core. The high resolution oxygen isotope record of the core was established by Chang (1997). The same planktonic foraminifera *G. inflata* was also utilized for oxygen isotope measurement because of the abundance of this species in the region (B'e, 1977). The oxygen isotope record of the core was then compared with the orbitally-tuned, stacked, standard oxygen isotope record from Martinson et al. (1987), and control points of the oxygen isotope record were thus identified. Precise correlation with the current data base proved difficult, but the comparison enabled identification of the boundaries of isotope stages 1/2, 2/3, and 3/4 at 73.5 cm, 136 cm, and 348.5 cm, respectively. The control points were then used to establish the stratigraphic framework below 110 cm of the core.

Sedimentation rates of the core were calculated on the basis of the calibrated AMS ^{14}C dates. The calculated sedimentation rates are 7.8 cm/kyr for the Holocene period (3.5 cm to 73.5 cm), and 7.4 cm/kyr for the last glacial maximum (73.5 cm to 108.5 cm). Based on the oxygen isotope stratigraphy (Chang, 1997), the average sedimentation rate of the core from the top down to 26 m is approximately 5 cm/kyr.

3.2 Radioisotope Records

The depth profiles of ^{238}U and ^{232}Th concentrations for the MD962085 core are presented in Figure 2. A low concentration of ^{238}U (ranging from ~0.3 to 0.6 dpm/g) was found in the uppermost sediments, while remarkably high ^{238}U concentrations (ranging from >1.9 to ~4.5 dpm/g) were found throughout the rest of the core between 73.5 and 400 cm (Table 1, Figure 2). According to AMS ^{14}C age and oxygen isotope stratigraphy, this sharp increase in U concentration corresponds to the boundary between oxygen isotope stages 1 and 2. Then, these values remained high throughout the last glacial period.

In contrast to U ^{238} concentrations, ^{232}Th exhibited low activities ranging from ~ 0.4 to 0.8 dpm/g throughout the core. ^{232}Th is one of the most particle-reactive elements, and is the only non-radiogenic isotope of Th. In the ocean, ^{232}Th is essentially locked in the lattice structure of minerals, and derived entirely from continents through eolian and riverine pathways. Therefore, the low concentrations of ^{232}Th in the MD962085 core indicate a small input of lithogenic material into the deep-sea sediments where it located. The relatively low contents of terrigenous material (calculated from the residual fraction of total sedimentary components subtracting the %opal+%$CaCO_3$+%TOC; Yu, unpublished data) in this core are consistent with this explanation. Although ^{232}Th activities in the core are low, they still displayed variations corresponding to the glacial-interglacial climate change (Table 1, Figure 2). These variations are due to enhanced terrigenous material input from the Orange River and greater input of

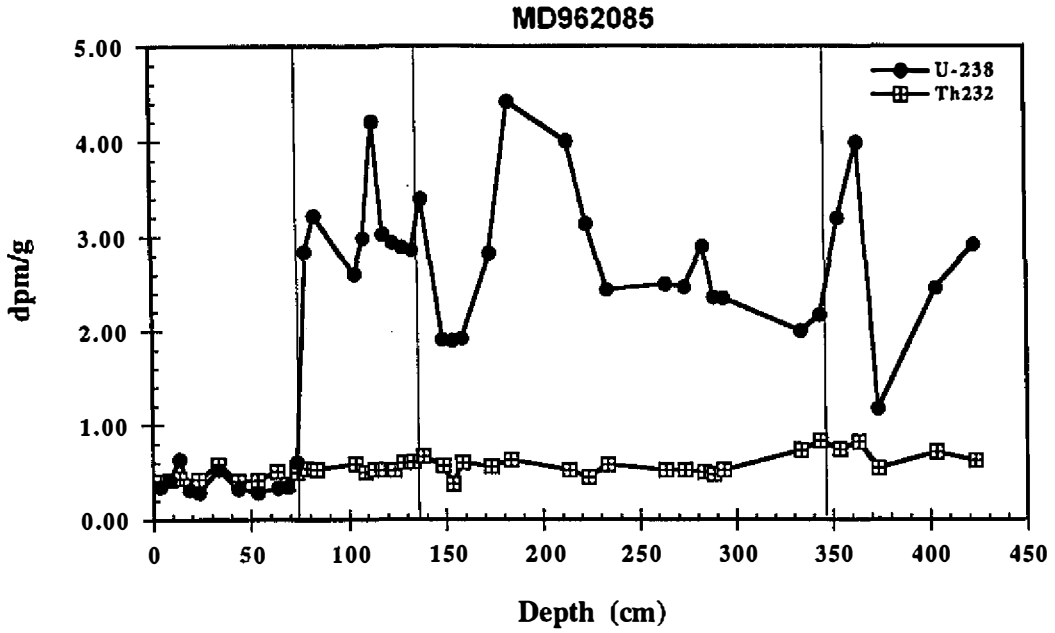

Fig. 2. Uranium-238 and Thorium-232 activity profiles in the MD962085 core. The vertical lines delineate the core sections corresponding to oxygen isotope stage 2, 3, and 4, respectively.

eolian dust during the low stands of sea level and drier condition during the glacial period .

3.3 Authigenic U Profile

High ^{238}U and low ^{232}Th concentrations of samples during the last glacial period in the MD962085 core indicate that both authigenic and lithogenic U existed in the sediments. Since only total U content of the sediments can be measured, it is necessary to derive the authigenic U contents of these samples by an indirect means. Virtually all of the ^{232}Th in marine sediments are lithogenic, and typical $^{238}U/^{232}Th$ activity ratios for major crustal rocks and pelagic marine sediments are in the range of 0.8±0.2 (Anderson, 1982; Anderson et al., 1989; Wedepohl, 1995). Therefore, detrital ^{238}U can be estimated from ^{232}Th activities, and authigenic U content of sediments is calculated by the difference between measured total ^{238}U activity and detrital ^{238}U activity as

$$\text{Authigenic U} = U_m - (0.8\pm0.2) * {}^{232}Th_m$$

where $^{238}U_m$ and $^{232}Th_m$ are the measured ^{238}U and ^{232}Th content respectively, and (0.8±0.2) * $^{232}Th_m$ represents the estimation of the mean activity of detrital ^{238}U in dpm/g (Anderson et al., 1989). The results, displayed as % authigenic U, are shown in Figure 3a. Clearly, high activity ratio of $^{238}U/^{232}Th$ existed between 73.5 and 400 cm of the core (Table 1), and a large

fraction of the uranium (Figure 3a) found during the whole last glacial period in this core is not detrital; rather, the additional U is authigenic.

3.4 Implications for the Authigenic Uranium Enrichment in the Glacial Sediments

Enhanced concentrations of uranium in deep-sea sediments have been recognized on hydrothermally active mid-ocean ridges (MORs; Fisher and Bostrom, 1969; Bender et al., 1971), and also in reduced sediments (Cochran and Krishnaswami, 1980; Barnes and Cochran, 1990; Klinkhammer and Palmer, 1991). Due to the remoteness of this core from any hydrothermal inputs, it is unlikely that hydrothermal activity is the causative factor of U enrichments observed in MD962085. Rather, additional U observed in the core may have been added to the sediments as a result of reducing conditions either in the sediment deposited during last glacial period or within the water column.

Generally, the large fraction of authigenic U must have been added to the sediment as a result of two processes: (1) biogenic fixation of U in the water column and scavenging of U by microorganisms, or precipitation of U from solution as discrete U minerals or adsorption as a hydrolyzed species to the surface of existing minerals or by reducing conditions in microenvironments within settling particles (Fisher et al., 1987; Anderson, 1982; Anderson et al., 1989) and (2) U precipitation at the water-sediment interface where higher proportions of reactive organic matter may enhance bacterial activity, which acts as a trap for uranium either directly (Mann and Fyfe, 1984) or indirectly by lowering the redox potential during the early diagensis of organic matter (Cochran and Krishnaswami, 1980; Barnes and Cochran, 1990; Klinkhammer and Palmer, 1991). Indeed, both processes are major mechanisms of U incorporation into anoxic organic-rich marine sediments. When reducing conditions occur close to the sediment-water interface, additional U is added to the sediments from the water column through the steps of the reduction of the soluble U(VI) in the overlying sea water, the removal of the soluble U (VI) from the bottom water or the pore water of the sediments, and precipitation of the insoluble U(IV) as the solid phase uranium in the sediment. A pore water gradient is thus created from the sediment-water interface down to the deeper depths of the sediment (Cochran and Krishnaswami, 1980; Barnes and Cochran, 1990; Klinkhammer and Palmer, 1991), and the removal of uranium into the solid phase thus affects the sedimentary record. This removal process leads marine sediments to a substantial sink for the uranium dissolved in seawater. The authigenic uranium added to the sediments by this process accumulates at a rate which is established by pore water U concentration gradient, which depends on the level of oxygen in the bottom water and the flux of metabolizable organic matter from both export production, which originates from the water above, and accumulation rate which is supplied laterally (i.e., sediment focusing). Lacking pore water U profile and other data to allow further investigation on the variation in level of oxygen in bottom water, in the following we attempt only to examine how the variations in flux of organic matter account for additional U uptake in the sediments deposited during the last glacial period of the MD962085 core. %TOC of the core is analyzed, and used to calculate $^{230}Th_{ex}$-normalized TOC flux to represent the relative supplies of organic matter from the overlying sea water in the region where the core is collected.

From the results, the variations in % authigenic U (Figure 3a) are observed to correspond

well to the variations in %TOC of the MD962085 core (Figure 3b). The sharp increase in authigenic U at circa 12 kyr BP also coincides with the sharp increase in %TOC. Values for both authigenic U and %TOC remain high for the last full glacial period, i.e.. stages 2 to 4. In addition, the variations in $^{230}Th_{ex}$-normalized TOC flux were consistent with those in both %TOC and authigenic U (Figure 3c).

$^{230}Th_{ex}$-normalized TOC flux was calculated by normalizing TOC flux to $^{230}Th_{ex}$ activity in sediments. $^{230}Th_{ex}$-normalized flux method was first proposed by Bacon (1984), and has been discussed extensively elsewhere (Suman and Bacon, 1989; Francois et al., 1990). Since first proposed, the method has been applied heavily in paleoceanographic studies (e.g., Francois et al., 1990; 1993; Kumar et al., 1993; Yu, 1994, 1996). This method is based on observations from sediment trap studies suggesting that annually averaged fluxes of excess ^{230}Th ($^{230}Th_{ex}$) to the seafloor are nearly constant and close to the expected rates of production from the radioactivity decay of ^{234}U dissolved in the overlying water column (Yu, 1994). Thus, $^{230}Th_{ex}$ can be used as a reference against which the flux (F_i) of other sedimentary components can be estimated:

$$F_i = \beta * z * f_i/[^{230}Th_{ex}{}^0]$$

where β is the production rate of ^{230}Th in the water column, z is the water depth, f_i is the weight fraction of component i in the sediment, and $^{230}Th_{ex}{}^0$ is the activity of excess ^{230}Th (i.e. ,scavenging ^{230}Th) decay corrected to time of deposition using an independent time scale based on ^{14}C or $\delta^{18}O$ stratigraphy. By normalizing to $^{230}Th_{ex}{}^0$, each measurement gives a flux estimate at each sampled point and thus allows better time resolution. It has been proven that the $^{230}Th_{ex}$-normalized paleoflux method can correct the influence of post-depositional sediment redistribution by bottom current or sediment winnowing (Suman et al., 1989; Francois, et al., 1990). Thus, it can provide better estimates of preserved particle rain rate on the sea floor (e.g., Suman et al., 1989; Francois, et al., 1990; 1993; Kumar et al., 1993).

The higher levels of both %TOC and $^{230}Th_{ex}$-normalized TOC flux in the same sequence with depth of the MD962085 core indicate higher paleoproductivity during the last full glacial period, including oxygen isotope stage 2, 3 and 4, than that during the Holocene in the study region (Figure 3b and c). These observations support the interpretation of high authigenic U may have added to the sediment as a result of more U fixation in or association with biogenic materials is scavenged. Alternatively, the dissolved U is added to sediments in its diagenetic sequence when more labile organic carbon is consumed at the sediment-water interface. The decomposition of more organic matter caused higher oxygen consumption, and led to the development of reducing conditions being closer to the sediment water interface. More labile organic carbon in the sediment is produced by a higher settling flux of biogenic materials from the overlying water column. The higher flux of the biogenic materials may result from more intensive upwelling of the Benguela upwelling system during the glacial periods. Intensive upwelling brought deep nutrient-rich waters to the ocean surface, and provided more nutrient for the planktonic communities in the surface water. The higher paleoproductivity during the last glacial period in this core is also suggested by Chang (1997) from his data on the higher abundance of planktonic foraminifera.

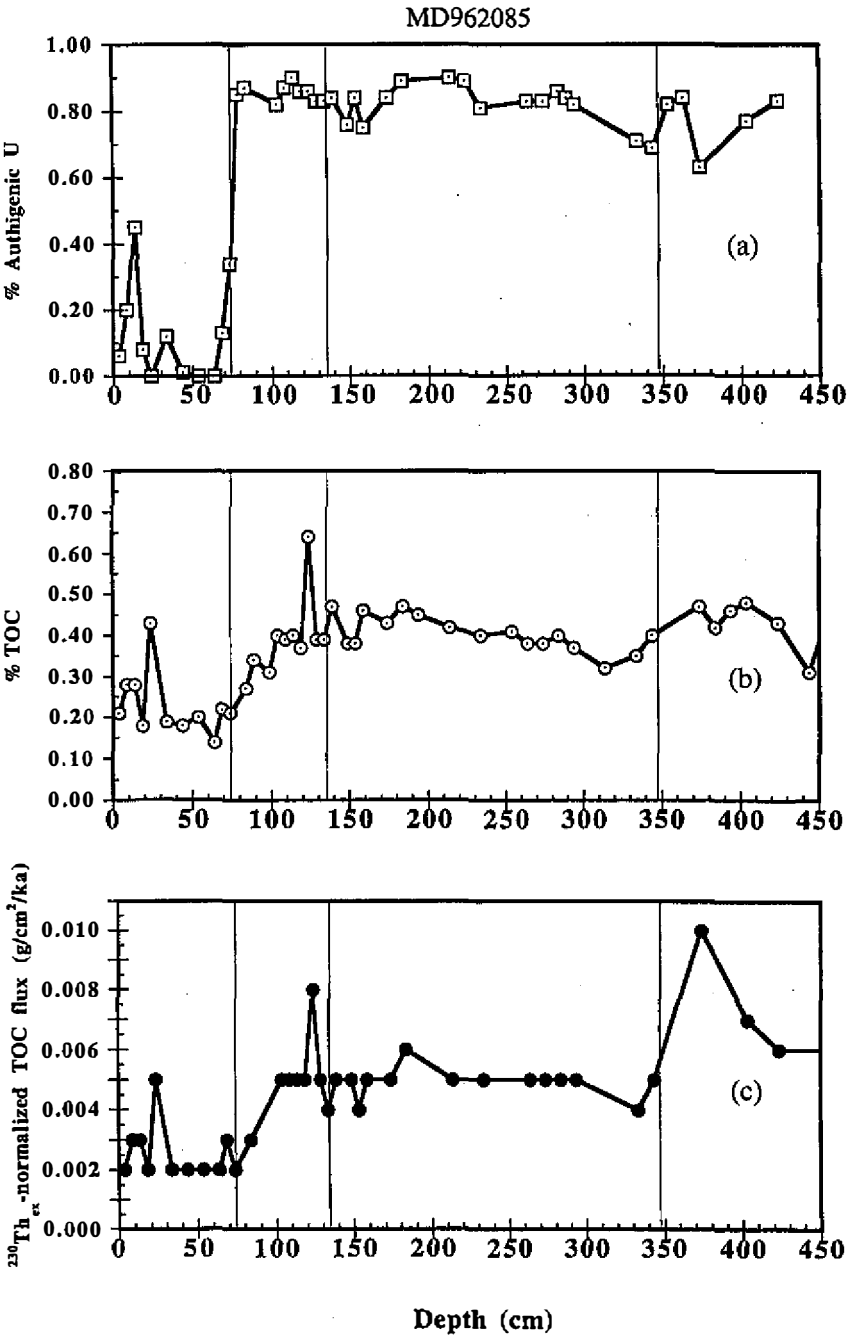

Fig. 3. (a) Profiles of calculated % authigenic U; (b) measured data of %TOC; and (c) $^{230}Th_{ex}$-normalized TOC flux of the MD962085 core. The vertical lines delineate the core sections corresponding to oxygen isotope stage 2, 3, and 4, respectively.

In deep-sea sediments, the roles of "organic activity" in the water column and of early diagensis of organic carbon are difficult to weigh (Hillaire-Marcel et al., 1990). However, the uranium dissolved in sediment pore water is often characterized by high $^{234}U/^{238}U$ ratios (as high as 1.23±0.03; Cochran and Krishnaswami, 1980) compared to those for uranium dissolved in the water column. Uranium dissolved in seawater has a typical $^{234}U/^{238}U$ activity ratio of 1.14 (Chen et al., 1986) whereas weathered lithogenic material often has a ratio < 1.0 due to preferential leaching of the radiogenic ^{234}U. Thus, the relatively high $^{234}U/^{238}U$ activity ratios with an average of 1.10±0.04 (1 σ for 30 analytical data) measured in the sediment sections over the last glacial period of this core (Table 1) support the explanation of "organic activity" in the water column. However, more accurate measurement of the $^{234}U/^{238}U$ activity ratio by mass spectrometry is needed to elucidate the argument.

A similar pattern, with high $^{238}U/^{232}Th$ activity ratios in sediment deposited during the high productivity period, has been observed off the present-day NW African upwelling area (Mangini and Diester-Haass, 1983), in the Labrador Sea (Hillaire-Marcel et al., 1990), and in the north of the Polar Frontal Zone (Francois et al., 1993). High authigenic U from the last glacial stage in the sediments from the northeast Atlantic Ocean was also found, but it was interpreted differently. Cores from Cape Verde Rise and Porcupine Abyssal Plain showed anomalously high U contents in sediments laid down during the last glacial stage (radiocarbon age 12-24 kyr B. P.; Thomson et al., 1990). All the cores exhibit maximum Mn levels and maximum U levels in the same sequence with increasing depth in cores. However, no correlation is observed between authigenic U and organic carbon contents of these cores. Thomson and his colleagues (1990) suggested that the U enrichment is not syngenetic with the deposition of its host glacial age sediments but is, rather, an early diagenetic addition. The position of the U peak is a result of the glacial stage/Holocene decrease in sediment accumulation rate and subsequent deepening of the oxic/post-oxic boundary into the glacial age sediments during Holocene pelagic deposition (Thomson et al., 1990). In the MD962085 core, no difference in terms of mean sedimentation rates between the last glacial stage and the Holocene was found. Thus, as already discussed in the previous section of this paper, the higher paleoproductivity due to more intensive upwelling of the Benguela upwelling system may be the major cause of high authigenic U concentrations during the last full glacial stage in this region.

Although glacial high levels of authigenic U in the MD962085 core are largely caused by high export flux of organic material, the oxygen concentration in the water columns may play an additional role in enhancing this high level phenomenon. The O_2-depleted gyre water of the Angola Current (Visser, 1969), and more intensive upwelling activity of the Benguela upwelling system during the glacial periods may have caused the reduced condition to develop not only at the bottom water-sediment interface, but also in the water column and in microenvironments in the settling particles. To prove whether this alternative process is an important mechanism for the removal of uranium from sea water into the sediments, an experiment examining the uranium content of particulate matter collected with sediment traps is needed.

Acknowledgments This study was supported by Grant NSC87-2611-M-003-001- from the National Science Council of the Republic of China and by National Taiwan Normal University. The authors would like to thank Dr. C.-H. Wang, Institute of Earth Sciences, Academia

Sinica, for assisting in collection of CO_2 gas from samples for AMS ^{14}C dating. Comments by Dr. C.-A. Huh and an anonymous reviewer have improved this paper, and their efforts are greatly appreciated.

REFERENCES

Anderson, R. F., 1982: Concentration, vertical flux, and remineralization of particulate uranium in seawater. *Geochim. Cosmochim. Acta*, **52**, 1557-1569.

Anderson, R. F. and A. P. Fleer, 1982: Determination of natural actinides and plutonium in marine particulate material. *Analy. Chem.*, **54**, 1142-1147.

Anderson, R. F., A. P. Lehuray, M. Q. Fleisher and J. W. Murray, 1989: Uranium deposition in Saanich Inlet sediments, Vancouver Island. *Geochim. Cosmochim. Acta*, **53**, 2205-2213.

Bacon, M. P., 1984: Glacial to interglacial changes in carbonate and clay sedimentation in the Atlantic ocean estimated from Th-230 measurements. *Isot. Geosci.*, **2**, 97-111.

Bard, E., B. Hamelin, R. G. Fairbanks and A. Zindler, 1990: Calibration of the ^{14}C timescale over the past 30,000 years using mass spectrometric U-Th ages from Barbados corals. *Nature*, **345**, 405-410.

Barnes, C. E. and J. K. Cochran, 1990: Uranium removal in oceanic sediments and oceanic U balance. *Earth Planet. Sci. Lett.*, **97**, 94-101.

B'e, A. W. H., 1977: An ecological, zoogeographic and taxonomic review of recent planktonic foraminifera. *Oceanic Micropalaeontology*, **1**, 1-100.

Bender, M, W. S. Broecker, V. Gornitz, U. Middel, R. Kay, S.-S. Sun and P. Biscaye, 1971: Geochemistry of three cores from the East Pacific Rise. *Earth Planet. Sci. Lett.*, **12**, 425-433.

Broecker, W. S. and T.-H. Peng, 1982: Tracers in the Sea, Eldigio Press, Palisades, New York, 689pp.

Broecker, W. S., M. Andree, G. Bonani, W. Wolfli, M. Klas, A. Mix and H. Oeschger, 1988: Comparison between radiocarbon ages obtained on coexisting planktonic foraminifera. *Paleoceanogr.*, **6**, 647-657.

Chang, F.-Y., S.-J. Kao and K.-K. Liu, 1991: Analysis of organic and carbonate carbon in sediments. *Acta Oceanogr. Taiwanica*, **27**, 140-150.

Chang, Z.-B., 1997: Late Quaternary high-resolution planktonic foraminifer stable isotope and faunal assemblage record of the South Benguela Current. Master's degree dissertation, National Taiwan Ocean University, Keelung, Taiwan, ROC.

Chen, J. H., R. L. Edwards and G. J. Wasserburg, 1986: ^{238}U, ^{234}U and ^{232}Th in seawater. *Earth Planet. Sci. Lett.*, **80**, 241-251.

Cochran, J. K. and S. Krishnaswami, 1980: Radium, thorium, uranium and Pb-210 in deep-sea sediments and sediment pore waters from the North Equatorial Pacific. *Am. J. Sci.*, **280**, 849-889.

Cochran, J. K., A. E. Carey, E. R. Scholkovitz and L. D. Suppenant, 1986: The geochemistry of uranium and thorium in coastal marine sediments and sediment pore waters. *Geochim.*

Cosmochim. Acta, **50**, 663-680.

Colley, S., J. Thomson, and J. Toole, 1989: Uranium relocations and derivation of quasi-isochrons for a turbidite/pelagic sequence in the Northeast Atlantic. *Geochim. Cosmochim. Acta*, **53**,1223-1234.

Colley, S., J. Thomson, 1985: Recurrent uranium relocations in distal turbidites emplaced in pelagic conditions. *Geochim. Cosmochim. Acta*, **49**, 2339-2348.

Diester-Haass, L., 1985: Late Quaternary sedimentation on the eastern Walvis Ridge, SE Atlantic (HPC 532 and 4 piston cores). *Mar. Geol.*, **65**, 145-189.

Fisher, D. E. and K. Bostrom, 1969: Uranium rich sediments on the East Pacific Rise. *Nature*, **224**, 64-65.

Fisher, D. E., J.-L. Teyssie, S. Krishnaswami and M. Baskaran, 1987: Accumulation of Th, Pb, U, and Ra in marine phytoplankton and its geochemical significance. *Limnol. Oceanog.*, **32**, 131-142.

Francois, R., M. P. Bacon and D. Suman, 1990: Thorium-230 profiling in deep-sea sediments: high resolution records of flux and dissolution of carbonate in the equatorial Atlantic during the last 24,000 years. *Paleoceanogr.*, **5**, 761-787.

Francois, R., M. P. Bacon, M. Altabet and L. D. Labeyrie, 1993: Glacial/interglacial changes in sediment rain rate in the SW Indian sector of subantarctic waters as recorded by ^{230}Th, ^{231}Pa, U and δ^{15}N. *Paleoceanogr.*, **8**, 611-629.

Hedges, J. I. and J. H. Stern, 1984: Carbon and nitrogen determinations of carbonate-containing solids. *Liminol. Oceanogr.*, **29**, 657-663.

Hillaire-Marcel, C., A. Aksu, C. Causse, A. de Vernal and B. Ghaleb, 1990: Response of Th/U in deep Labrador Sea sediments (ODP site 646) to changes in sedimentation rates and paleoproductivity. *Geol.*, **18**, 162-165.

Klinkhammer, G. and M. R. Palmer, 1991: Uranium in the oceans:where it goes and why. *Geochim. Cosmochim. Acta*, **55**, 1799-1806.

Ku, H. H., 1966: Notes on the use of propagation of error formulas. *J. Res. Nat. Bur. Strand. Sect.* **C**, 263-273.

Kumar, N., Gwiazda, R., Anderson, R.F. and Froelich, P.N., 1993: ^{231}Pa/^{230}Th ratios in sediments as a proxy for past changes in Southern Ocean productivity. *Nature*, **362**, 45-47.

Mann, H. and W. S. Fyfe, 1984: An experimental study of algal uptake of U, Ba, V, Co and Ni from dilute solutions. *Chem. Geol.*, **44**, 385-398.

Mangini, A. and L. Diester-Haass, 1983: Excess Th-230 in sediments off N.W. Africa traces upwelling in the past, Coastal Upwelling: Its record part A: Responses of the sedimentary regime to present coastal upwelling, Plenum, New York, 455-470pp.

Martinson, D. G., N. G. Pisias, J. D. Hays, J. Imbrie, T. C. Moore and N. J. Shackleton, 1987: Age dating and the orbital theory of the ice ages: development of a high resolution 0 to 300,000 year chronostratigraphy. *Quat. Res.*, **27**, 1-29.

Nelson, G. and L. Hutchings, 1983: The Benguela upwelling area. *Prog. Oceanogr.*, **12**, 333-356.

Oberhansli, H., 1991: Upwelling signals at the northeastern Walvis Ridge during the past 500,000 years. *Paleoceanogr.*, **6**, 53-71.

Shannon, L. V., 1985: The Benguela ecosystem part I: Evolution of the Benguela, physical feature and processes. *Oceanogr. Mar. Bio. Ann. Rev.*, **23**, 105-182.

Siesser, W. G., 1978: Aridification of the Namibia desert: Evidence from oceanic cores, Antarctic glacial history and world paleoenvironments. *A. A. Balkema, Rotterdam*, 105-114.

Stramma, L. and R. G. Peterson, 1990: Geostrophic transport in the Benguela Current region. *J. Phys. Oceanogr.*, **19**, 1440-1448.

Stuiver, M. and P. J. Reimer, 1993: Extended ^{14}C data base and revised Calib 3.0 ^{14}C age calibration program. *Radiocarbon*, **35**,215-230.

Suman, D. O. and M. P. Bacon, 1989: Variations in Holocene sedimentation in the North American Basin determined from Th-230 measurements. *Deep-Sea Res.*, **36**, 869-878.

Thomson J., H. E. Wallace, S. Colley and J. Toole, 1990: Authigenic Uranium in Atlantic sediments of the last glacial stage - a diagenetic phenomenon. *Earth Planet. Sci. Lett.*, **98**, 222-232.

Wallace H. E., J. Thomson, T. R. S. Wilson, P. P. E. Weaver, N. C. Higgs and D. J. Hydes, 1988: Active diagenetic formation of metal-rich layers in N.E. Atlantic sediments. *Geochim. Cosmochim. Acta*, **52**, 1557-1569.

Visser, G. A., 1969: The oxygen-minimum layer between the surface and 1000 m in the north-eastern South Atlantic. *Bull. Div. Sea Fish. South Africa*, **6**, 10-22.

Wedepohl, K. H., 1995: The composition of the continental crust. *Geochim. Cosmochim. Acta*, **59**, 1217-1232.

Yu, E.-F., 1994: Variations in the particulate flux of ^{230}Th and ^{231}Pa and paleoceanographic applications of the $^{231}Pa/^{230}Th$ ratio. Ph.D. Thesis, Massachusetts Institute of Technology/Woods Hole Oceanographic Institution, MA, USA.

Yu, E.-F., R. Francois and M. P. Bacon, 1996: Similar rates of modern and last-glacial ocean thermohaline circulation inferred from radiochemical data. *Nature*. **379**, 689-694.